

Cross-correlation effects in the solution NMR spectra of near-equivalent spin-1/2 pairs

James W. Whipham,¹ Gamal Moustafa,¹ Mohamed Sabba,¹ Weidong Gong,¹ Christian Bengs,¹ and Malcolm H. Levitt¹

Department of Chemistry, University of Southampton, SO17 1BJ, UK

(*Electronic mail: mhl@soton.ac.uk)

(Dated: 22 August 2022)

The NMR spectra of spin-1/2 pairs contains four peaks, with two inner peaks much stronger than the outer peaks in the near-equivalence regime. We have observed that the strong inner peaks have significantly different linewidths, when measurements were performed on a $^{13}\text{C}_2$ -labelled triyne derivative. This linewidth difference may be attributed to strong cross-correlation effects. We develop the theory of cross-correlated relaxation in the case of near-equivalent homonuclear spin-1/2 pairs, in the case of a molecule exhibiting strongly anisotropic rotational diffusion. Good agreement is found with the experimental NMR lineshapes.

I. INTRODUCTION

If a nuclear spin system is perturbed from a thermal equilibrium state, it slowly returns to equilibrium through nuclear spin relaxation. Such relaxation processes are driven by fluctuations in the interactions between the nuclear spins and the thermal molecular environment. In general, many types of fluctuating interaction are involved, and these interactions may be correlated with each other. For example, in solution NMR, the fluctuations of nuclear spin interactions are caused by random molecular tumbling, and since the rotation of a molecule modulates all intramolecular interactions at the same time, the fluctuations of these interactions are correlated. Such cross-correlation effects are well-documented in solution NMR¹⁻⁸. Cross-correlation gives rise to differential line broadening and line narrowing, and differences in the longitudinal relaxation behaviour of individual multiplet components^{1-4,6,8}. Cross-correlation effects have been used to estimate the relative orientations of nuclear spin interaction tensors, allowing the estimation of molecular torsional angles⁹⁻¹¹. A particularly important set of cross-correlation effects is associated with the so-called TROSY techniques (transverse relaxation-optimized spectroscopy), which have important applications, especially in biomolecular NMR^{12,13}.

Cross-correlation often takes place between the fluctuations of internuclear dipole-dipole (DD) couplings and chemical shift anisotropy (CSA) interactions. Such DD-CSA cross-correlation effects are well-known for heteronuclear spin pairs, and underpin important techniques such as TROSY^{4,12,13}. In this paper we demonstrate strong DD-CSA cross-correlation effects in the solution NMR of a system containing *homonuclear* pairs of ^{13}C nuclei, in the limit of *near-magnetic-equivalence*, implying that the chemical shift difference between the coupled nuclear sites is much smaller than the internuclear J-coupling.

The system of interest is the $^{13}\text{C}_2$ -labelled triyne derivative referred to here as **I**, which has the following systematic name: 1-methoxy-4-((4-methoxymethoxy)phenyl)hexa-1,3,5-triyn-1-yl)benzene. Its molecular structure is shown in figure 1a. Each molecule of **I** has a rod-like shape, with two ^{13}C labels at the central pair of carbon atoms, in the cen-

tre of the triyne moiety. The two end groups are different, endowing the two ^{13}C nuclei with slightly different chemical shifts ($\Delta\delta = 0.16$ ppm). Since the ^{13}C - ^{13}C J-coupling is large ($J_{\text{CC}} = 214.15$ Hz), the ^{13}C pair is in the near-equivalent regime at all accessible magnetic fields¹⁴.

The ^{13}C NMR spectrum of a 0.3 M solution of **I** in CDCl_3 is shown in figure 2. This corresponds to the expected AB four-peak structure, although the two outer peaks are too weak to be observed. The two strong central peaks are only partially resolved, and form a strongly asymmetric lineshape, as shown by the inset in figure 2. As discussed below, the asymmetry of the central peak pair is due to strong DD-CSA cross-correlation effects.

An analysis of cross-correlated relaxation in **I** must take into account its rod-like shape, which causes strongly anisotropic rotational diffusion in solution. The theory of nuclear spin relaxation has been developed in the context of model-free treatments of biomolecules with anisotropic internal motions¹⁵⁻²⁰. However, most existing treatments of cross-correlated relaxation in small molecules assume approximately isotropic rotational diffusion, which is clearly not applicable here. In the following sections we develop the theory of cross-correlated relaxation in systems with anisotropic rotational diffusion. We provide analytical formulae for the NMR spectrum of a near-equivalent homonuclear spin pair undergoing cross-correlated relaxation in the presence of anisotropic rotational diffusion. The observed spectral asymmetry is reproduced, with good agreement between theory, experiment and numerical simulations.

II. EXPERIMENTAL

A. Sample

The synthesis of **I** is described in the supplementary material. 19 mg of **I** was made up to a 200 μL 0.3 M solution in CDCl_3 . 5 freeze-thaw degassing cycles were performed on the solution.

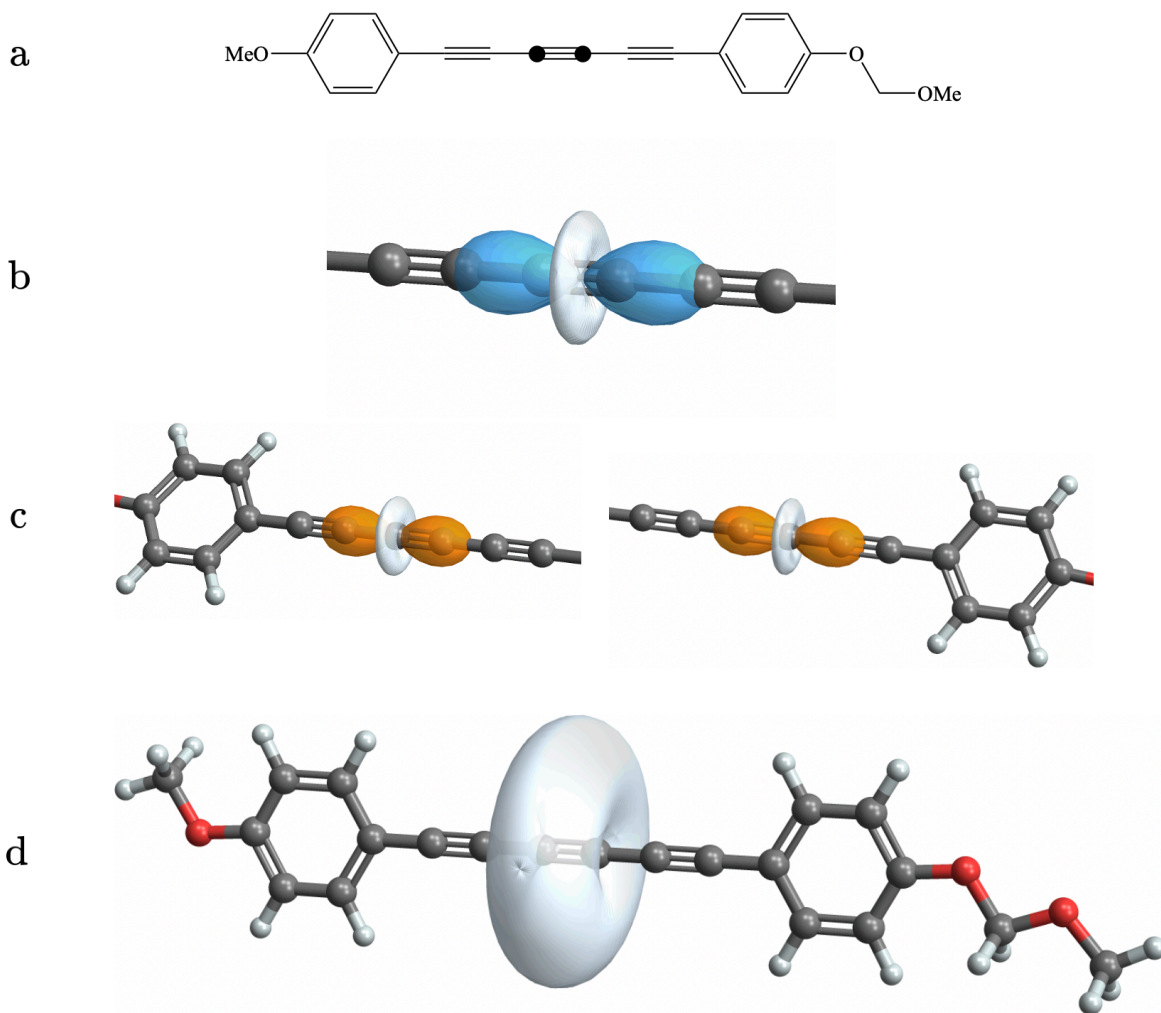


FIG. 1. (a) Molecular structure of **I**, with ^{13}C labelled sites depicted by black circles; (b) The rank-2 part of the ^{13}C - ^{13}C dipole-dipole coupling tensor, represented by an ovaloid^{21,22}; (c) The calculated ^{13}C CSA tensors of the ^{13}C labels represented by ovaloids; (d) The inertia tensor of the molecule, represented as an ovaloid, superimposed on the molecular structure. The grey atoms are C, the red atoms O, and white H. The graphics were generated in *SpinDynamica*²³.

B. NMR

The experiments were performed on a 400 MHz (9.4 T) Bruker Avance Neo spectrometer. The pulse sequence was a simple 90° pulse-acquire. The ^{13}C nutation frequency was 6.68 kHz and 1 scan was performed. The NMR signal was sampled with 131 k data points with a spectral width of 81.46 ppm.

C. Computational chemistry

Geometry optimisation and simulation of the magnetic shielding tensors of **I** were performed at the B3LYP/aug-cc-PVTZ²⁴⁻²⁶ level of theory in the Gaussian 09 suite of programs²⁷. After geometry optimisation, the dipole-dipole cou-

pling tensor between the two ^{13}C nuclei was calculated from the internuclear distance. The parameters obtained from the computations are presented in table I.

III. THEORY

A. Anisotropic rotational diffusion

To analyze the relaxation behaviour of this system, **I** is approximated as a rigid molecule undergoing anisotropic rotational diffusion in solution, and is presented in the vein of Huntress^{28,29}. We treat the molecule as a rod-shaped symmetric top, corresponding to a strongly anisotropic inertia tensor depicted by the ovaloid^{21,22} shown in figure 1d, with a rotational diffusion tensor coincident with the inertia tensor.

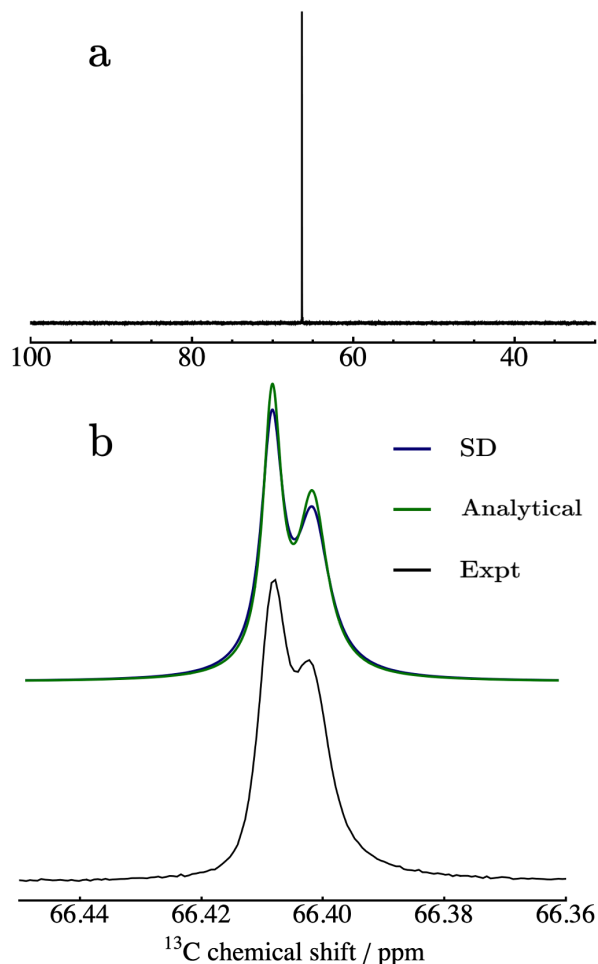


FIG. 2. ^{13}C spectra of a 0.3 M solution of **I** in CDCl_3 , at a magnetic field of 9.4 T. (a) Overview of the ^{13}C spectrum; (b) Black line: Expanded view of the central doublet, showing the strongly asymmetric linewidths of the doublet components. Dark blue line: Numerical *SpinDynamica* simulation²³, using the theory given in the text and parameters in table I. Green line: Superposition of two Lorentzians with amplitudes, frequencies, and linewidths specified by table V and eq. (53).

The ovaloid representation of the inertia tensor, shown in figure 1d, has the form of a dimpled disk, or a doughnut with an incomplete hole. This shape may be interpreted as follows: Take a vector starting from the molecular centre of mass, and pointing in any direction. The vector intersects the ovaloid surface at some point. The distance from the centre of mass to the intersection point is proportional to the moment of inertia for a rotation around that vector. Rotations around an axis which is perpendicular to the long axis of the molecule are associated with a large moment of inertia, so that the surface is relatively distant from the centre of mass. A rotation around the long axis, on the other hand, has a small moment of inertia, so that the surface is close to the origin in that direction. Hence the ovaloid has the appearance of a dimpled disk, with the dimples along the long axis of the molecule.

The principal axis system of the rotational diffusion tensor

TABLE I. Spin system parameters for **I** in solution.

Parameter	Value	Note
J_{jk}	214.15 Hz	Experimental ^a
$\Delta\delta_{\text{iso}}$	0.16 ppm	Experimental ^b
$b_{jk}/(2\pi)$	-4152.84 Hz	Estimated ^c
$\{\alpha_{PD}^{jk}, \beta_{PD}^{jk}, \gamma_{PD}^{jk}\}$	$\{0, -2.5, 0\}^\circ$	Frames obtained by diagonalising calculated tensors
δ_j^{CSA}	-145.7 ppm	Calculated
η_j	0.020	Calculated
$\{\alpha_{PD}^j, \beta_{PD}^j, \gamma_{PD}^j\}$	$\{0, -2.6, 0\}^\circ$	Frames obtained by diagonalising calculated tensors
δ_k^{CSA}	-145.4 ppm	Calculated
η_k	0.023	Calculated
$\{\alpha_{PD}^k, \beta_{PD}^k, \gamma_{PD}^k\}$	$\{0, -2.6, 0\}^\circ$	Frames obtained by diagonalising calculated tensors
τ_\perp	136.5 ps	Estimated from the parameters in this table and experimental T_1

^a Obtained from 90° pulse-acquire spectrum on a 700 MHz spectrometer. ^b Estimated from the ^{13}C spectrum of natural abundance material; ^c Estimated from the internuclear distance, $r_{jk} = 122$ pm.

is denoted D and is depicted in figure 3. A laboratory reference frame L may be defined such that its z-axis is aligned with the external magnetic field (see figure 3). The relative orientation of the D and L frames may be described by using the Euler angle triplet $\Omega_{DL} = \{\alpha_{DL}, \beta_{DL}, \gamma_{DL}\}$. In this article, the z-y-z convention for Euler angles is used throughout³⁰. Due to the molecular tumbling, these Euler angles are in general stochastic functions of time, $\Omega_{DL} = \Omega_{DL}(t)$, since the D -frame is molecule-fixed whilst the L -frame is space-fixed.

The stochastic time-dependence of the Euler angles Ω_{DL} may be expressed in terms of the time-correlation functions of the rank- l Wigner D-matrices:

$$\begin{aligned}
 G_{mm'mm'}^{ll'}(t_0, \tau) &= \overline{D_{mn}^{(l)}(\Omega_{DL}(t_0)) D_{m'n'}^{(l')*}(\Omega_{DL}(t_0 + \tau))} \\
 &= \int \int d\Omega_{DL}(t_0) d\Omega_{DL}(t_0 + \tau) \\
 &\quad \times D_{mn}^{(l)}(\Omega_{DL}(t_0)) D_{m'n'}^{(l')*}(\Omega_{DL}(t_0 + \tau)) \\
 &\quad \times P(\Omega_{DL}(t_0)) P(\Omega_{DL}(t_0 + \tau) | \Omega_{DL}(t_0))
 \end{aligned} \tag{1}$$

where $P(\Omega_{DL}(t_0)) = (8\pi^2)^{-1}$ is the probability density that the molecule hosting the spin system will be at orientation $\Omega_{DL}(t_0)$ at time $t = t_0$, and $P(\Omega_{DL}(t_0 + \tau) | \Omega_{DL}(t_0))$ is the conditional probability that the molecule will be at orientation $\Omega_{DL}(t_0 + \tau)$ at time $t = t_0 + \tau$, given that it was at orientation $\Omega_{DL}(t_0)$ at time $t = t_0$. If the stochastic process is assumed to be stationary, these probabilities are independent of t_0 , allowing the arbitrary choice of time origin $t_0 = 0$. The expression

for the conditional probability is given by Favro³¹, and is,

$$P(\Omega_{DL}(\tau)|\Omega_{DL}(0)) = \sum_V \psi_V^*(0)\psi_V(\tau)e^{-E_V\tau}, \quad (2)$$

where $\psi_V(t)$ are eigenfunctions of the operator $H_{\text{rot diff}} = \mathbf{L} \cdot \mathbf{D} \cdot \mathbf{L}$, with corresponding eigenvalues E_V , where \mathbf{L} and \mathbf{D} are the angular momentum vector and the diffusion tensor, respectively. For a symmetric top, we may write,

$$H_{\text{rot diff}} = D_{\perp}(L_x^2 + L_y^2) + D_{\parallel}L_z^2, \quad (3)$$

where D_{\perp} and D_{\parallel} are rotational diffusion constants associated with axes perpendicular and parallel, respectively, with the molecular long axis. Note that eq. (3) is written in the D -frame.

Eq. (3) is of the same form as the rigid-rotor Hamiltonian for a symmetric-top. As such, the eigenfunctions and eigenvalues in eq. (2) are those of a quantum mechanical rigid-rotor^{32,33}:

$$\psi_V(t) \rightarrow \phi_{K,M}^J(t) \equiv (-1)^{M-K} \sqrt{\frac{2J+1}{8\pi^2}} D_{-M-K}^{(J)}(\Omega(t)) \quad (4)$$

$$E_V \rightarrow E_K^J \equiv D_{\perp}J(J+1) + K^2(D_{\parallel} - D_{\perp}). \quad (5)$$

For our specific system, we will see that $J \equiv l = 2$ and $K = 0$. The only non-vanishing term in the correlation function is then $E_0^{(2)} = 6D_{\perp}$, and related to the rotational correlation time $\tau_{\perp} \equiv (6D_{\perp})^{-1}$. Rotational motion around the molecular long axis does not modulate the interactions responsible for relaxation. This is a consequence of the coincidence of the P - and D -frames. The secularised time-correlation function becomes,

$$G_{mm'}^l(\tau) = G_{mm'nn'}^{ll'}(0, \tau) = \delta_{ll'} \delta_{mm'} \frac{(-1)^{n+n'}}{2l+1} e^{-\tau/\tau_{\perp}}. \quad (6)$$

B. Coherent Hamiltonian

The coherent spin Hamiltonian describes those spin interactions which are the same for all members of the spin ensemble at a given point in time. For a homonuclear spin-1/2 pair in solution, it may be written in the rotating frame of the Zeeman interaction as,

$$H_{\text{coh}} = \frac{1}{2}\omega_{\Sigma}(I_{1z} + I_{2z}) + \frac{1}{2}\omega_{\Delta}(I_{1z} - I_{2z}) + \omega_J \mathbf{I}_1 \cdot \mathbf{I}_2, \quad (7)$$

with

$$\begin{aligned} \omega_{\Sigma} &= \omega_1 + \omega_2 \\ \omega_{\Delta} &= \omega_1 - \omega_2 \\ \omega_J &= 2\pi J_{12}, \end{aligned} \quad (8)$$

where J_{12} is the isotropic part of the spin-spin coupling tensor, and ω_j is the precession frequency of spin I_j ,

$$\omega_j = \omega_0(1 + \delta_j^{\text{iso}}) - \omega_{\text{rf}}. \quad (9)$$

Here, ω_0 is the Larmor frequency of the isotope, δ_j^{iso} is the isotropic chemical shift for the j^{th} spin, and ω_{rf} is the radiofrequency carrier frequency.

The Hamiltonian may be diagonalised by using the perturbed singlet-triplet basis, \mathbb{B}'_{ST} , defined as,

$$\mathbb{B}'_{\text{ST}} = \{|S'_0\rangle, |T'_{+1}\rangle, |T'_0\rangle, |T'_{-1}\rangle\}, \quad (10)$$

with elements,

$$\begin{aligned} |S'_0\rangle &= \cos\frac{\theta}{2}|S_0\rangle - \sin\frac{\theta}{2}|T_0\rangle \\ |T'_{+1}\rangle &= |T_{+1}\rangle \\ |T'_0\rangle &= \sin\frac{\theta}{2}|S_0\rangle + \cos\frac{\theta}{2}|T_0\rangle \\ |T'_{-1}\rangle &= |T_{-1}\rangle, \end{aligned} \quad (11)$$

where the singlet and triplet states are given by,

$$\begin{aligned} |S_0\rangle &= \frac{1}{\sqrt{2}}(|\alpha\beta\rangle - |\beta\alpha\rangle) \\ |T_{+1}\rangle &= |\alpha\alpha\rangle \\ |T_0\rangle &= \frac{1}{\sqrt{2}}(|\alpha\beta\rangle + |\beta\alpha\rangle) \\ |T_{-1}\rangle &= |\beta\beta\rangle, \end{aligned} \quad (12)$$

and θ is the *singlet-triplet mixing angle*, defined by,

$$\tan\theta = \omega_{\Delta}/\omega_J. \quad (13)$$

The eigenvalues of H_{coh} are,

$$\begin{aligned} \omega_{S'_0} &= -\frac{1}{4}(\omega_J + 2\omega_e) \\ \omega_{T'_{+1}} &= +\frac{1}{4}(\omega_J + 2\omega_{\Sigma}) \\ \omega_{T'_0} &= -\frac{1}{4}(\omega_J - 2\omega_e) \\ \omega_{T'_{-1}} &= +\frac{1}{4}(\omega_J - 2\omega_{\Sigma}), \end{aligned} \quad (14)$$

where,

$$\omega_e^2 = \omega_{\Delta}^2 + \omega_J^2. \quad (15)$$

These eigenvalues are used in section III E to analyse the signal, allowing assignment of coherence-peak correspondence.

C. Fluctuating Hamiltonian

The fluctuating Hamiltonian is a sum of contributions from the anisotropic spin interactions. These interactions differ between ensemble members at a given point in time, due to the random molecular tumbling. The current analysis is restricted to the intra-pair dipole-dipole (DD) and chemical shift anisotropy (CSA) interactions,

$$H_{\text{fluc}} = H_{\text{DD}} + H_{\text{CSA}}, \quad (16)$$

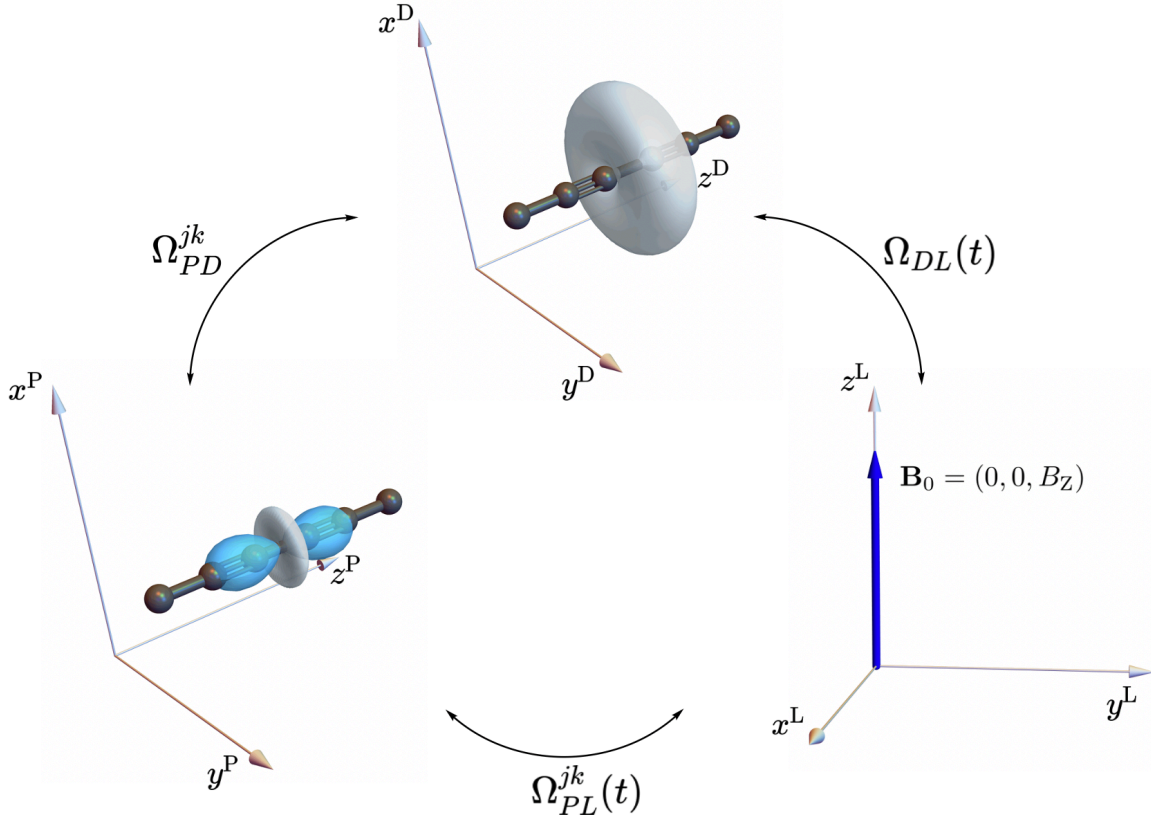


FIG. 3. Relevant frame transformations illustrated using the DD-tensor as an example. On the left, the coordinate system is the molecule-fixed P -frame of the DD interaction, with the z -axis parallel to the internuclear vector. The set of angles Ω_{PD}^{jk} orientate the P - and D -frames. The molecule-fixed D -frame is given by the principal axis frame of the inertia tensor with its z -axis parallel to the molecular long axis. The laboratory frame L is defined such that its z -axis is parallel to the applied magnetic field. The angles $\Omega_{DL}(t)$ orient the D - and L -frames with respect to each other. These angles are time-dependent, since the L -frame is space-fixed and stochastic molecular tumbling continuously alters the orientation of the D - and L -frames with respect to one another. The angles parameterising the transformation between the P - and L -frames will be time-dependent for the same reason.

as well as the cross-correlation between the two mechanisms.

The spin Hamiltonian for interaction Λ may be written in terms of irreducible spherical tensor operators as³⁴,

$$H_{\Lambda}(t) = c_{\Lambda} \sum_{l=0}^{+2} \sum_{m=-l}^{+l} A_{lm}^{\Lambda*}(t) X_{lm}^{\Lambda}, \quad (17)$$

where c_{Λ} is an interaction-dependent constant, $A_{lm}^{\Lambda}(t)$ are time-dependent components of a spatial spherical tensor, and X_{lm}^{Λ} are components of a spin or spin-field spherical tensor.

Spatial spherical tensors may be transformed between arbitrary reference frames F and G by using the Wigner matrices and the Euler angles relating the two frames:

$$\left[A_{lm}^{\Lambda} \right]^G = \sum_{m'=-l}^{+l} \left[A_{lm'}^{\Lambda} \right]^F D_{m'm}^{(l)}(\Omega_{FG}) \quad (18)$$

This process may be repeated for a chain of any number of reference frames. Figure 3 depicts the transformations from the principal axis frame of a spin interaction to the laboratory frame. The laboratory-frame spatial components acquire

a stochastic time-dependence through the motional modulation of the Euler angles $\Omega_{DL}(t)$, representing the rotational diffusion of the molecules in solution.

1. Direct dipole-dipole coupling.

In the case of the dipole-dipole interaction between spins I_j and I_k ($\Lambda = jk$), the tensor components X_{2m}^{jk} are equal to the rank-2 spherical tensor spin operators,

$$X_{2m}^{jk} = T_{2m}^{jk}, \quad (19)$$

as given in the laboratory frame in table III. Assuming a rigid molecular geometry, the interaction constant for the dipole-dipole coupling is given by,

$$c_{jk} = b_{jk} = - \left(\frac{\mu_0}{4\pi} \right) \hbar \gamma_j \gamma_k r_{jk}^{-3}, \quad (20)$$

where r_{jk} is the internuclear distance. In the current case, the ^{13}C - ^{13}C internuclear distance of $r_{jk} = 122$ pm corresponds to

a direct dipole-dipole coupling of $b_{jk}/(2\pi) = -4152.84$ Hz.

The principal axis system P^{jk} of the dipole-dipole coupling tensor is aligned such that its z-axis is along the ^{13}C - ^{13}C internuclear vector (see figure 3). In general, the relative orientation of the dipole-dipole principal axis system and the molecular diffusion tensor is defined by an Euler angle triplet $\Omega_{PD}^{jk} = \{\alpha_{PD}^{jk}, \beta_{PD}^{jk}, \gamma_{PD}^{jk}\}$, as shown in figure 3. In the current case, the rod-like geometry of the molecule causes near-coincidence of the principal axis systems of the ^{13}C - ^{13}C dipole-dipole coupling and that of the inertia tensor, so that the angle β_{PD}^{jk} is very small.

The rank-2 spherical tensor representing the spatial part of the dipole-dipole interaction has the following components in its principal axis frame:

$$[A_{2m}^{jk}]^P = \sqrt{6} \delta_{m0} \quad (21)$$

where δ_{ab} is the Kronecker-delta.

2. Chemical-shift anisotropy.

In the case of the chemical shift anisotropy of spin I_j ($\Lambda = j$), spin-field tensors X_{lm}^j of ranks $l = 1$ and $l = 2$ are formed by coupling the rank-1 spherical tensor spin operators T_{1m}^j with the rank-1 spherical components of the external magnetic field⁸:

$$X_{lm}^j = \sum_{m', m''} C_{mm'm''}^{l11} T_{1m'}^j B_{1m''} \quad (22)$$

where $C_{mm'm''}^{l11}$ are Clebsch-Gordon coefficients³⁵. Explicit expressions for the case $l = 2$ are given in the laboratory frame in table III.

The magnetic shielding tensors are given in the supplementary material. From these, the *Haeberlen convention*³⁶ is used to define the anisotropy and biaxiality parameters, respectively, as,

$$\delta^{\text{CSA}} = \delta_{zz}^P - \delta^{\text{iso}} \quad (23)$$

and,

$$\eta = \frac{\delta_{xx}^P - \delta_{yy}^P}{\delta^{\text{CSA}}}, \quad (24)$$

with tensor components defined by,

$$|\delta_{zz}^P - \delta^{\text{iso}}| \geq |\delta_{xx}^P - \delta^{\text{iso}}| \geq |\delta_{yy}^P - \delta^{\text{iso}}|. \quad (25)$$

Values of these parameters are given in table I.

D. Relaxation Superoperator

The semi-classical relaxation superoperator takes the form,

$$\hat{\Gamma}(t) = - \int_{-\infty}^0 d\tau \overline{\hat{H}_{\text{fluc}}(0) \hat{H}_{\text{fluc}}(\tau)}, \quad (26)$$

TABLE II. Irreducible spherical spatial tensor components for $l = 2$, $p = 0$ in their principal axis frame³⁷

Interaction, Λ	c^Λ	$[A_{20}^\Lambda]^P$
DD, spins I_j and I_k	b_{jk}	$\sqrt{6}$
CSA, spin I_j	$-\gamma_j$	$\sqrt{\frac{3}{2}} \delta_j^{\text{CSA}}$

TABLE III. Irreducible spherical spin and spin-field tensor components for $l = 2$ in the L-frame³⁷

Interaction, Λ	m	$[X_{2m}^\Lambda]^L$
	0	$\frac{1}{2\sqrt{6}} (4I_{jz}I_{kz} - I_j^- I_k^+ - I_j^+ I_k^-)$
DD, spins I_j and I_k	± 1	$\mp \frac{1}{2} (I_j^\pm I_{kz} + I_{jz} I_k^\pm)$
	± 2	$\frac{1}{2} (I_j^\pm I_k^\pm)$
	0	$\sqrt{\frac{2}{3}} B_0 I_{jz}$
CSA, spin I_j	± 1	$\mp \frac{1}{2} B_0 I_j^\pm$
	± 2	0

where $\hat{H}_{\text{fluc}}(t)$ is the fluctuating Hamiltonian commutation superoperator in the interaction representation of the Zeeman Hamiltonian, defined by the transformation,

$$\hat{H}_{\text{fluc}}(t) = \exp(i\hat{H}_Z t) \hat{H}_{\text{fluc}}(0) \exp(-i\hat{H}_Z t), \quad (27)$$

and the overbar denotes an ensemble average.

To describe the relaxation effects giving rise to the asymmetric line shapes in figure 2, the interaction constants and irreducible spherical spin and spatial tensor components in table II are used. By eq. (16), the relaxation superoperator may be written as a sum over auto- and cross-correlated mechanisms as,

$$\begin{aligned} \hat{\Gamma} &= \sum_{\Lambda, \Lambda'} \hat{\Gamma}^{\Lambda\Lambda'} \\ &= \hat{\Gamma}^{\text{DD}} + \hat{\Gamma}^{\text{CSA}} + \hat{\Gamma}^{\text{DD} \times \text{CSA}}, \end{aligned} \quad (28)$$

Using eq. (17), the relaxation superoperator for rank- l interactions Λ and Λ' becomes,

$$\hat{\Gamma}_l^{\Lambda\Lambda'} = -c^\Lambda c^{\Lambda'} \sum_m J_{lm}^{\Lambda\Lambda'}(\omega_0) [\hat{X}_{lm}^\Lambda]^L [\hat{X}_{lm}^{\Lambda'}]^\dagger, \quad (29)$$

with spectral density functions given in our case by,

$$\begin{aligned} J_{lm}^{\Lambda\Lambda'}(\omega_0) &= [A_{ln}^{\Lambda*}]^D [A_{ln'}^{\Lambda'}]^D \int_{-\infty}^0 d\tau G_{mm'nn'}^{ll'} e^{-im'\omega_0|\tau|} \\ &= \sum_{mm'} \frac{(-1)^{n+n'}}{2l+1} [A_{ln}^{\Lambda*}]^D [A_{ln'}^{\Lambda'}]^D \frac{\tau_{\perp}}{1+m^2\omega_0^2\tau_{\perp}^2}. \end{aligned} \quad (30)$$

where $[A_{ln}^{\Lambda}]^D$ are n^{th} -components of l^{th} -rank irreducible spherical tensors in the diffusion frame, and τ_{\perp} is the rotation correlation time about an axis perpendicular to the molecular long axis. The components $[A_{ln}^{\Lambda}]^D$ are known in the P -frame and may be expressed in the D -frame using the transformation in eq. (18).

E. Liouvillian

The evolution of the spin ensemble is described by the *Liouville-von Neumann equation*, which may be expressed as,

$$\frac{d}{dt}|\rho(t)\rangle = \hat{\mathcal{L}}(t)|\rho(t)\rangle, \quad (31)$$

where $|\rho(t)\rangle$ is the ensemble-averaged density operator, and $\hat{\mathcal{L}}$ is the Liouvillian, itself given by,

$$\hat{\mathcal{L}}(t) = -i\hat{H}_{\text{coh}}(t) + \hat{\Gamma}(t), \quad (32)$$

where $\hat{H}_{\text{coh}}(t)$ is the coherent Hamiltonian commutation superoperator defined by,

$$\hat{H}_{\text{coh}}(t)|Q\rangle = [H_{\text{coh}}(t), Q]. \quad (33)$$

If the Hilbert space of the spin system has dimension N_{H} , then the corresponding operator (Liouville) space has dimension $N_{\text{L}} = N_{\text{H}}^2$. It follows that the Liouvillian has a set of N_{L} eigenvalues and eigenoperators,

$$\hat{\mathcal{L}}|Q_q\rangle = \Lambda_q|Q_q\rangle \quad q \in \{0, 1, \dots, N_{\text{L}} - 1\}, \quad (34)$$

with,

$$\Lambda_q = -\lambda_q + i\omega_q, \quad (35)$$

where λ_q and ω_q are both real. In the case where $\omega_q \neq 0$, the eigenoperators correspond to quantum coherences (QC) which decay with rate constant λ_q and oscillate at frequency ω_q . Eigenoperators with real eigenvalues ($\omega = 0$) represent a particular configuration of spin state populations with decay rate constant λ_q .

F. NMR spectrum

1. Signal

The signal may be written in terms of the eigenvalues of eq. (35) as³⁸,

$$s(t) = \sum_q a_q e^{\Lambda_q t}, \quad (36)$$

TABLE IV. Coherence eigenoperators of \hat{H}_{coh} along with the associated eigenfrequencies and peak amplitudes.

$ Q_q\rangle$	ω_q	a_q
$ S'_0\rangle\langle T'_{+1} $	$\frac{1}{2}(\omega_{\Sigma} + \omega_J + \omega_e)$	$\frac{1}{2}\sin^2\frac{\theta}{2}$
$ T'_{-1}\rangle\langle S'_0 $	$\frac{1}{2}(\omega_{\Sigma} - \omega_J - \omega_e)$	$\frac{1}{2}\sin^2\frac{\theta}{2}$
$ T'_0\rangle\langle T'_{+1} $	$\frac{1}{2}(\omega_{\Sigma} + \omega_J - \omega_e)$	$\frac{1}{2}\cos^2\frac{\theta}{2}$
$ T'_{-1}\rangle\langle T'_0 $	$\frac{1}{2}(\omega_{\Sigma} - \omega_J + \omega_e)$	$\frac{1}{2}\cos^2\frac{\theta}{2}$

with a_q the peak amplitude given by,

$$a_q = (Q_{\text{obs}}|Q_q)(Q_q|\hat{U}_{\text{exc}}|\rho_{\text{eq}}), \quad (37)$$

where \hat{U}_{exc} is the total propagator for the excitation sequence and $|\rho_{\text{eq}}\rangle$ is the thermal equilibrium density operator. In quadrature detection, $|Q_{\text{obs}}\rangle \approx -\frac{1}{2}ie^{i\phi_{\text{rec}}}|I^- \rangle$ with ϕ_{rec} being the receiver phase. Since the experiment here is a 90° pulse-acquire, we make the approximation,

$$\hat{U}_{\text{exc}}|\rho_{\text{eq}}\rangle = \hat{R}_x(\pi/2)I_z = -I_y, \quad (38)$$

ignoring constant numerical factors.

Non-vanishing peak amplitudes are associated with (-1) -quantum eigenoperators $|Q_q\rangle$, as defined by the eigenequation:

$$\hat{I}_z|Q_q\rangle = -|Q_q\rangle \quad (39)$$

where \hat{I}_z is the commutation superoperator of the angular momentum operator I_z .

In the absence of relaxation, these observable operators are the (-1) -quantum eigenoperators of the commutation superoperator \hat{H}_{coh} and are given by elements of the basis,

$$\begin{aligned} \mathbb{B}_Q = \{ & ||S'_0\rangle\langle T'_{+1}|, ||T'_{-1}\rangle\langle S'_0|, \\ & ||T'_0\rangle\langle T'_{+1}|, ||T'_{-1}\rangle\langle T'_0| \}, \end{aligned} \quad (40)$$

which is a subset of the 16-element basis of all outer products of elements in \mathbb{B}'_{ST} .

In the absence of relaxation, the Liouvillian eigenvalues are purely imaginary, and are given by $\Lambda_q = +i\omega_q$, where ω_q are the peak frequencies. These are given in general by

$$\omega_q = -(\omega_r - \omega_s), \quad (41)$$

with $r, s \in \{S'_0, T'_{+1}, T'_0, T'_{-1}\}$, as given in table IV.

The two eigenoperators corresponding to (-1) -quantum coherences between the perturbed triplet states are particularly important in the current context, since these coherences give rise to the two components of the spectral doublet shown

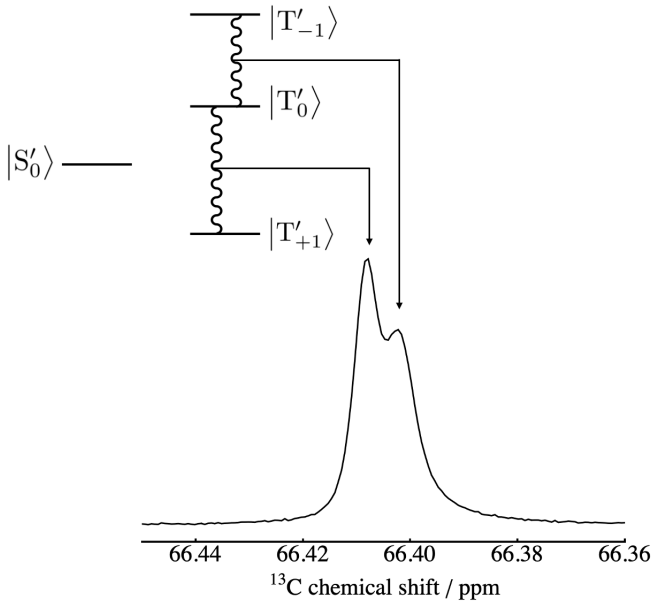


FIG. 4. The correspondence between the single-quantum triplet-triplet coherences (wiggly lines) and the NMR spectrum. The coherence represented by the operator Q_+ is associated with the narrow peak while the coherence represented by Q_- is associated with the broad peak.

in figure 2, as can be seen from their amplitudes in table IV. These two eigenoperators are denoted as follows:

$$\begin{aligned} Q_+ &= |T'_0\rangle\langle T'_{+1}| \\ Q_- &= |T'_{-1}\rangle\langle T'_0| \end{aligned} \quad (42)$$

The corresponding Liouvillian eigenvalues are as follows:

$$\Lambda_{\pm} = -\lambda_{\pm} + i\omega_{\pm} \quad (43)$$

In general, the superoperators \hat{H}_{coh} and $\hat{\Gamma}$ do not commute. The presence of the relaxation superoperator $\hat{\Gamma}$ may therefore modify both the eigenvalues and the eigenoperators of the Liouvillian $\hat{\mathcal{L}}$. Indeed the modification of the peak frequencies by relaxation effects has been documented in the literature in a different context³⁹. In the current case, the eigenvalues of the (-1) -quantum eigenoperators are only slightly modified by the relaxation superoperator. This is because the off-diagonal elements of the (-1) -quantum Liouvillian block are much smaller than the corresponding eigenvalue differences, as discussed in the Supporting Information. Hence, in the following discussion, we assume that the (-1) -quantum eigenoperators of the full Liouvillian, including relaxation, are given to a good approximation by the operators in equation 40.

The correspondence between the two triplet-triplet coherences and the NMR spectrum is depicted in figure 4.

2. Frequencies

The coherence frequencies are given by the imaginary parts of the Liouvillian eigenvalues. As shown in the Supporting

Information, the off-diagonal parts of the (-1) -quantum Liouvillian block may be ignored. With this approximation, the coherence frequencies are as specified in Table IV. The frequencies of the two triplet-triplet coherences are given by

$$\omega_{\pm} = \frac{1}{2}(\omega_{\Sigma} \pm \omega_J \mp \omega_e) \quad (44)$$

The splitting between the two inner peaks is given by,

$$\Delta\omega = \omega_- - \omega_+ = \omega_e - \omega_J \simeq \frac{\omega_{\Delta}^2}{2\omega_J}. \quad (45)$$

where the approximation applies to the near-equivalence regime.

3. Linewidths

Since the off-diagonal elements of $\hat{\Gamma}$ are small in the basis \mathbb{B}_Q , relative to the corresponding differences in the diagonal elements, the real parts of the Liouvillian eigenvalues are given by

$$\text{Re}(\Lambda_q) \simeq \frac{(Q_q|\hat{\Gamma}|Q_q)}{(Q_q|Q_q)} \quad (46)$$

where the Liouville bracket is defined by⁴⁰,

$$(Q_q|Q_{q'}) = \text{Tr}\{Q_q^{\dagger}Q_{q'}\}. \quad (47)$$

The real positive quantities $\lambda_q = -\text{Re}(\Lambda_q)$ may be interpreted as the coherence decay rate constants for the eigenoperators $|Q_q\rangle$. After Fourier transformation of the NMR spectrum, the peak associated with the eigenoperator $|Q_q\rangle$ has amplitude a_q , centre frequency ω_q , and has a Lorentzian shape with half-width-at-half-height equal to λ_q , in units of rad s^{-1} . Its full-width-at-half-height is given by λ_q/π in units of Hz.

The relaxation superoperator $\hat{\Gamma}$ may be written as a sum of auto-correlation terms for the DD and CSA interactions, and a DD \times CSA cross-correlation term (eq. (28)). The coherence decay rate constants λ_q may therefore be written as a superposition of terms:

$$\lambda_q = \lambda_q^{\text{DD}} + \lambda_q^{\text{CSA}} + \lambda_q^{\text{DD}\times\text{CSA}}. \quad (48)$$

The computed CSA biaxiality parameters η are very small for both ^{13}C sites of the system **I** (see table I). Making the approximation that $\eta_j \simeq \eta_k \simeq 0$, all components of the spatial tensor associated with the CSA interaction vanish except for $[A_{20}^{\text{CSA}}]^P = \sqrt{3/2}\delta^{\text{CSA}}$, and the transformation in eq. (18) reduces to,

$$\begin{aligned} [A_{2n}^{\text{CSA}}]^D &= [A_{20}^{\text{CSA}}]^P D_{0n}^{(2)}(\Omega_{PD}^j) \\ &= [A_{20}^{\text{CSA}}]^P, \end{aligned} \quad (49)$$

where the last line is obtained by noting that the P - and D -frames are coincident, and all Euler angles may be set to zero.

For the two triplet-triplet coherences, each term in eq. (48) is given by,

$$\lambda_{\pm}^{\text{DD}} = \frac{3}{20} b_{jk}^2 \tau_{\perp} \left(3 + \frac{3}{1 + \omega_0^2 \tau_{\perp}^2} + \frac{2}{1 + 4\omega_0^2 \tau_{\perp}^2} \right), \quad (50)$$

$$\lambda_{\pm}^{\text{CSA}} = \frac{1}{20} \omega_0^2 \tau_{\perp} \left\{ \left([\delta_j^{\text{CSA}}]^2 + [\delta_k^{\text{CSA}}]^2 \right) \frac{5 + 2\omega_0^2 \tau_{\perp}^2}{1 + \omega_0^2 \tau_{\perp}^2} + \delta_j^{\text{CSA}} \delta_k^{\text{CSA}} \frac{3}{1 + \omega_0^2 \tau_{\perp}^2} \right\}, \quad (51)$$

and,

$$\lambda_{\pm}^{\text{DD} \times \text{CSA}} = \pm \frac{3}{20} \omega_0 b_{jk} \tau_{\perp} \left(\delta_j^{\text{CSA}} + \delta_k^{\text{CSA}} \right) \frac{3 + 2\omega_0^2 \tau_{\perp}^2}{1 + \omega_0^2 \tau_{\perp}^2}, \quad (52)$$

Equations (50) - (52) depend on the correlation time τ_{\perp} for molecular rotation around an axis perpendicular to the long axis of the molecule. Rotational diffusion *around* the molecular long axis does not modulate the spin interactions, under the approximation of a rigid symmetric top undergoing rotational diffusion, and does not lead to spin relaxation.

In the current case, the chemical shift anisotropies of the two spins are very similar, allowing the simplification $\delta_j^{\text{CSA}} \simeq \delta_k^{\text{CSA}} \simeq \delta_k^{\text{CSA}}$.

The limiting regimes of the correlation time τ_{\perp} are as follows:

1. In the *extreme narrowing limit*, $|\omega_0 \tau_{\perp}| \ll 1$, eq. (48) may be written,

$$\lambda_{\pm} \simeq \frac{3}{10} (4b_{jk} \pm 3\omega_0 \delta^{\text{CSA}}) b_{jk} \tau_{\perp} + \lambda^{\text{CSA}}, \quad (53)$$

where the CSA-induced decay rate constant λ^{CSA} is given by,

$$\lambda^{\text{CSA}} \simeq \frac{13}{20} \omega_0^2 [\delta^{\text{CSA}}]^2 \tau_{\perp}. \quad (54)$$

The field-dependence of the two rate constants λ_{\pm} is illustrated in figure 5a. The decay rate constant λ_{+} is minimized at a magnetic field such that $|4b_{jk}| = |3\omega_0 \delta^{\text{CSA}}|$, in which case the first term in eq. (53) cancels out. At this field, the dipole-dipole contribution to the decay rate constant vanishes, and λ_{+} becomes equal to the limiting CSA relaxation rate constant λ^{CSA} (eq. (54)). The decay rate constant λ_{+} , on the other hand, increases monotonically with increasing magnetic field.

2. In the *long correlation time limit*, $|\omega_0 \tau_{\perp}| \gg 1$, eq. (48) may be written as,

$$\lambda_{\pm} \simeq \frac{1}{20} (3b_{jk} \pm 2\omega_0 \delta^{\text{CSA}})^2 \tau_{\perp}. \quad (55)$$

The field-dependence of the two rate constants λ_{\pm} is illustrated in figure 5b. In this regime, the linewidth parameter λ_{+} goes to zero at a magnetic field such that $|3b_{jk}| = |2\omega_0 \delta^{\text{CSA}}|$. The strong narrowing of one of the two doublet components resembles the TROSY effects exploited in biomolecular NMR^{12,13}.

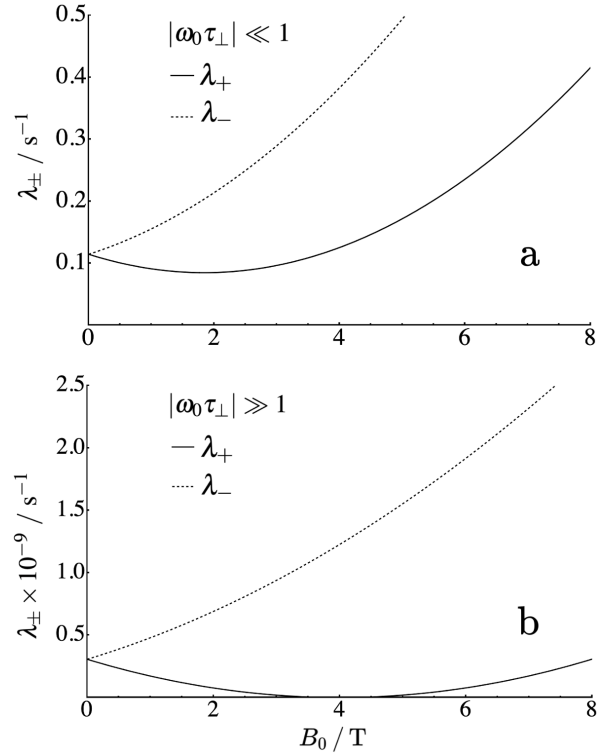


FIG. 5. Plots of the linewidth parameters λ_{\pm} against external static field, for the parameters in table I. (a) The extreme-narrowing limit, based on eq. (53), showing the minimum $\lambda_{+} = 8.47 \times 10^{-2} \text{ s}^{-1}$ at $B_0 = 1.84 \text{ T}$. (b) The long- τ_{\perp} limit, with a minimum $\lambda_{+} = 0$ at $B_0 = 4.0 \text{ T}$. The DD and CSA mechanisms cancel in the long- τ_{\perp} limit at this magnetic field. The cancellation is incomplete in the extreme-narrowing limit.

IV. RESULTS

Using eq. (37), the peak amplitudes associated with the (-1) -quantum singlet-triplet coherences are given by $\propto \sin^2(\theta/2)$, while those associated with the (-1) -quantum triplet-triplet coherences are given by $\propto \cos^2(\theta/2)$. In the current case, the singlet-triplet mixing angle is small ($\theta = -0.0750 = -4.30^\circ$), and the amplitudes are,

$$\begin{aligned} a_{S'_0 \rightarrow T'_{+1}} &= a_{T'_{-1} \rightarrow S'_0} \simeq 0.686 \times 10^{-3} \\ a_{T'_0 \rightarrow T'_{+1}} &= a_{T'_{-1} \rightarrow T'_0} \simeq 0.499, \end{aligned} \quad (56)$$

with the sum over all amplitudes equal to 1. The spectrum is therefore dominated by the strong peaks from the two triplet-triplet coherences.

From eqs. (15) and (44), the frequency ω_{+} is less than ω_{-} . This indicates that the left peak of the doublet is associated with the Q_{+} coherence, while the right-hand peak is associated with the Q_{-} coherence, after taking into account the sign of the Larmor frequency⁴¹. This assignment is shown in figure 4. The splitting between the peaks is given by $\Delta\omega/(2\pi) = 0.60 \text{ Hz}$.

From eqs. (50)-(52), since b_{jk} , ω_0 , δ_j^{CSA} and δ_k^{CSA} are all negative, we see that the cross-correlation contributions re-

TABLE V. Parameters used to plot the analytical spectral function in fig. 2.

Parameter	Value	Note
λ_+	0.583 s^{-1}	eq. (53)
λ_-	1.19 s^{-1}	eq. (53)
a_{\pm}	0.499	eq. (37)
ω_{\pm}	$\mp 1.90 \text{ rad s}^{-1}$	eq. (44)

duce the value of λ_+ while increasing the value of λ_- . For the experimental parameters, the coherence decay rate constants are given by $\lambda_+ \simeq 0.583 \text{ s}^{-1}$ and $\lambda_- \simeq 1.190 \text{ s}^{-1}$. These correspond to full peakwidths at half-height of 0.186 Hz and 0.379 Hz, for the left-hand and right-hand doublet components, respectively.

The green curve in figure 2 is a plot of the analytical spectral function

$$S(\omega) = a_+ \frac{\lambda_+}{\lambda_+^2 + (\omega - \omega_+)^2} + a_- \frac{\lambda_-}{\lambda_-^2 + (\omega - \omega_-)^2}, \quad (57)$$

using the parameters in table V. There is good agreement with the experimental ^{13}C NMR spectrum (black).

The blue curve in figure 2 shows the result of a numerical calculation using *SpinDynamica*²³ in which the full Liouvillian is diagonalized. There is good qualitative agreement between the numerical simulations, the analytical theory and the experimental result. The minor differences between the *SpinDynamica* simulation and the analytical theory may be attributed to the neglect of the off-diagonal Liouvillian elements in the analytical theory (see discussion after eq. (43)).

V. CONCLUSIONS

The results and theory reported here show that cross-correlated relaxation can have a strong effect on the NMR spectra of homonuclear spin-1/2 pairs in the near-equivalence regime. This has strong relevance to NMR experiments on long-lived states, which are often performed on spin systems of this kind^{42–45}.

In a following paper, we explore the influence of cross-correlated relaxation on the *longitudinal* relaxation of spin systems of this kind, including the relaxation of long-lived states.

ACKNOWLEDGEMENTS

We thank Laurynas Dagys for insightful discussions on both experiment and theory. This research was sup-

ported by the European Research Council (grant 786707-FunMagResBeacons) and EPSRC-UK (grants EP/P030491/1, EP/P009980/1). We also acknowledge the IRIDIS High Performance Computing Facility, and associated support services at the University of Southampton.

AUTHOR DECLARATIONS

Conflict of interest

The authors have no conflicts to disclose.

DATA AVAILABILITY STATEMENT

The data that support the findings of this study are available from the authors at reasonable request.

SUPPLEMENTARY INFORMATION

The derivation of the relaxation superoperator in more detail, and the synthesis details of **I** are in a document offered alongside the paper.

- ¹H. M. McConnell, “Effect of Anisotropic Hyperfine Interactions on Paramagnetic Relaxation in Liquids,” *J. Chem. Phys.* **25**, 709–711 (1956).
- ²H. Shimizu, “Theory of the Dependence of Nuclear Magnetic Relaxation on the Absolute Sign of Spin—Spin Coupling Constant,” *J. Chem. Phys.* **40**, 3357–3364 (1964).
- ³L. G. Werbelow and D. M. Grant, “Intramolecular Dipolar Relaxation in Multispin Systems,” *Adv. Magn. Reson.* **9**, 189 (1977).
- ⁴M. Goldman, “Interference effects in the relaxation of a pair of unlike spin-1/2 nuclei,” *Journal of Magnetic Resonance* (1969) **60**, 437–452 (1984).
- ⁵L. Di Bari, J. Kowalewski, and G. Bodenhausen, “Magnetization transfer modes in scalar-coupled spin systems investigated by selective two-dimensional nuclear magnetic resonance exchange experiments,” *J. Chem. Phys.* **93**, 7698–7705 (1990).
- ⁶A. Kumar, R. Christy Rani Grace, and P. K. Madhu, “Cross-correlations in NMR,” *Progress in Nuclear Magnetic Resonance Spectroscopy* **37**, 191–319 (2000).
- ⁷P. K. Madhu, P. K. Mandal, and N. Müller, “Cross-Correlation Effects Involving Curie Spin Relaxation in Methyl Groups,” *Journal of Magnetic Resonance* **155**, 29–38 (2002).
- ⁸J. Kowalewski and L. Mäler, *Nuclear Spin Relaxation in Liquids Theory, Experiments, and Applications*, 2nd ed. (CRC Press, Taylor & Francis Group, Boca Raton, FL, 2018).
- ⁹B. Reif, M. Hennig, and C. Griesinger, “Direct measurement of angles between bond vectors in high-resolution NMR,” *Science* **276**, 1230–1233 (1997).
- ¹⁰B. Reif, H. Steinhagen, B. Junker, M. Reggelin, and C. Griesinger, “Determination of the Orientation of a Distant Bond Vector in a Molecular Reference Frame by Cross-Correlated Relaxation of Nuclear Spins,” *Angew. Chem. Int. Ed.* **37**, 1903–1906 (1998).
- ¹¹S. Ravindranathan, X. Feng, T. Karlsson, G. Widmalm, and M. H. Levitt, “Investigation of Carbohydrate Conformation in Solution and in Powders by Double-Quantum NMR,” *J. Am. Chem. Soc.* **122**, 1102–1115 (2000).
- ¹²K. Pervushin, R. Riek, G. Wider, and K. Wüthrich, “Attenuated T2 relaxation by mutual cancellation of dipole–dipole coupling and chemical shift anisotropy indicates an avenue to NMR structures of very large biological macromolecules in solution,” *PNAS* **94**, 12366–12371 (1997).
- ¹³V. Tugarinov, P. M. Hwang, J. E. Ollerenshaw, and L. E. Kay, “Cross-Correlated Relaxation Enhanced 1H-13C NMR Spectroscopy of Methyl

- Groups in Very High Molecular Weight Proteins and Protein Complexes," *J. Am. Chem. Soc.* **125**, 10420–10428 (2003).
- ¹⁴M. C. D. Tayler and M. H. Levitt, "Singlet nuclear magnetic resonance of nearly-equivalent spins," *Phys. Chem. Chem. Phys.* **13**, 5556–5560 (2011).
- ¹⁵G. Lipari and A. Szabo, "Model-free approach to the interpretation of nuclear magnetic resonance relaxation in macromolecules. 1. Theory and range of validity," *J. Am. Chem. Soc.* **104**, 4546–4559 (1982).
- ¹⁶G. Lipari and A. Szabo, "Model-free approach to the interpretation of nuclear magnetic resonance relaxation in macromolecules. 2. Analysis of experimental results," *J. Am. Chem. Soc.* **104**, 4559–4570 (1982).
- ¹⁷L. K. Lee, M. Rance, W. J. Chazin, and A. G. Palmer, "Rotational diffusion anisotropy of proteins from simultaneous analysis of ¹⁵N and ¹³C α nuclear spin relaxation," *Journal of Biomolecular NMR* **9**, 287–298 (1997).
- ¹⁸M. Marcellini, M.-H. Nguyen, M. Martin, M. Hologne, and O. Walker, "Accurate Prediction of Protein NMR Spin Relaxation by Means of Polarizable Force Fields. Application to Strongly Anisotropic Rotational Diffusion," *J. Phys. Chem. B* **124**, 5103–5112 (2020).
- ¹⁹N. Tjandra, P. Wingfield, S. Stahl, and A. Bax, "Anisotropic rotational diffusion of perdeuterated HIV protease from ¹⁵N NMR relaxation measurements at two magnetic fields," *Journal of Biomolecular NMR* **8**, 273–284 (1996).
- ²⁰M. J. Osborne and P. E. Wright, "Anisotropic rotational diffusion in model-free analysis for a ternary DHFR complex," *Journal of Biomolecular NMR* **19**, 209–230 (2001).
- ²¹R. Radeglia, "On the pictorial representation of the magnetic screening tensor: Ellipsoid or ovaloid?" *Solid State Nuclear Magnetic Resonance* **4**, 317–321 (1995).
- ²²R. P. Young, C. R. Lewis, C. Yang, L. Wang, J. K. Harper, and L. J. Mueller, "TensorView: A software tool for displaying NMR tensors," *Magn. Reson. Chem.* **57**, 211–223 (2019).
- ²³C. Bengs and M. H. Levitt, "SpinDynamica: Symbolic and numerical magnetic resonance in a Mathematica environment," *Magn. Reson. Chem.* **56**, 374–414 (2018).
- ²⁴A. D. Becke, "Density-functional thermochemistry. I. The effect of the exchange-only gradient correction," *The Journal of Chemical Physics* **96**, 2155–2160 (1992).
- ²⁵T. H. Dunning, "Gaussian basis sets for use in correlated molecular calculations. I. The atoms boron through neon and hydrogen," *The Journal of Chemical Physics* **90**, 1007–1023 (1989).
- ²⁶R. A. Kendall, T. H. Dunning, and R. J. Harrison, "Electron affinities of the first-row atoms revisited. Systematic basis sets and wave functions," *The Journal of Chemical Physics* **96**, 6796–6806 (1992).
- ²⁷M. J. Frisch, G. W. Trucks, H. B. Schlegel, G. E. Scuseria, M. A. Robb, J. R. Cheeseman, G. Scalmani, V. Barone, G. A. Petersson, H. Nakatsuji, X. Li, M. Caricato, A. V. Marenich, J. Bloino, B. G. Janesko, R. Gomperts, B. Mennucci, H. P. Hratchian, J. V. Ortiz, A. F. Izmaylov, J. L. Sonnenberg, D. Williams-Young, F. Ding, F. Lipparini, F. Egidi, J. Goings, B. Peng, A. Petrone, T. Henderson, D. Ranasinghe, V. G. Zakrzewski, J. Gao, N. Rega, G. Zheng, W. Liang, M. Hada, M. Ehara, K. Toyota, R. Fukuda, J. Hasegawa, M. Ishida, T. Nakajima, Y. Honda, O. Kitao, H. Nakai, T. Vreven, K. Throssell, J. A. Montgomery, Jr., J. E. Peralta, F. Ogliaro, M. J. Bearpark, J. J. Heyd, E. N. Brothers, K. N. Kudin, V. N. Staroverov, T. A. Keith, R. Kobayashi, J. Normand, K. Raghavachari, A. P. Rendell, J. C. Burant, S. S. Iyengar, J. Tomasi, M. Cossi, J. M. Millam, M. Klene, C. Adamo, R. Cammi, J. W. Ochterski, R. L. Martin, K. Morokuma, O. Farkas, J. B. Foresman, and D. J. Fox, "Gaussian 09," (2016), Gaussian, Inc. Wallingford CT.
- ²⁸W. T. Huntress, "Effects of Anisotropic Molecular Rotational Diffusion on Nuclear Magnetic Relaxation in Liquids," *J. Chem. Phys.* **48**, 3524–3533 (1968).
- ²⁹W. T. Huntress, "The Study of Anisotropic Rotation of Molecules in Liquids by NMR Quadrupolar Relaxation," in *Advances in Magnetic and Optical Resonance*, Vol. 4, edited by J. S. Waugh (Academic Press, 1970) pp. 1–37.
- ³⁰Y. Millot and P. P. Man, "Active and passive rotations with Euler angles in NMR," *Concepts Magn. Reson.* **40A**, 215–252 (2012).
- ³¹L. D. Favro, "Theory of the Rotational Brownian Motion of a Free Rigid Body," *Phys. Rev.* **119**, 53–62 (1960).
- ³²R. N. Zare, *Angular Momentum: Understanding Spatial Aspects in Chemistry and Physics*, The George Fisher Baker Non-Resident Lectureship in Chemistry at Cornell University (Wiley, New York, 1988).
- ³³C. Wang, "Anisotropic-rotational diffusion model calculation of T₁ due to spin-rotation interaction in liquids," *Journal of Magnetic Resonance* (1969) **9**, 75–83 (1973).
- ³⁴S. A. Smith, W. E. Palke, and J. T. Gerig, "The Hamiltonians of NMR. part I," *Concepts Magn. Reson.* **4**, 107–144 (1992).
- ³⁵D. A. Varshalovich, A. N. Moskalev, and V. K. Khersonskii, *Quantum Theory of Angular Momentum* (World Scientific, Singapore, 1988).
- ³⁶U. Haeberlen, *High Resolution NMR in Solids: Selective Averaging*, Advances in Magnetic Resonance : Supplement No. 1 (Academic Press, New York, 1976).
- ³⁷S. A. Smith, W. E. Palke, and J. T. Gerig, "The Hamiltonians of NMR. Part II," *Concepts Magn. Reson.* **4**, 181–204 (1992).
- ³⁸R. R. Ernst, G. Bodenhausen, and A. Wokaun, *Principles of Nuclear Magnetic Resonance in One and Two Dimensions*, The International Series of Monographs on Chemistry No. 14 (Clarendon press, Oxford, 1992).
- ³⁹G. S. Harbison, "Interference between J-couplings and cross-relaxation in solution NMR spectroscopy: Consequences for macromolecular structure determination," *J. Am. Chem. Soc.* **115**, 3026–3027 (1993).
- ⁴⁰J. Jeener, "Superoperators in Magnetic Resonance," in *Advances in Magnetic and Optical Resonance*, Vol. 10 (Elsevier, 1982) pp. 1–51.
- ⁴¹M. H. Levitt, "The Signs of Frequencies and Phases in NMR," *Journal of Magnetic Resonance* **126**, 164–182 (1997).
- ⁴²G. Pileio, ed., *Long-Lived Nuclear Spin Order: Theory and Applications*, 1st ed. (Royal Society of Chemistry, S.I., 2020).
- ⁴³M. H. Levitt, "Singlet Nuclear Magnetic Resonance," *Annu. Rev. Phys. Chem.* **63**, 89–105 (2012).
- ⁴⁴G. Stevanato, J. T. Hill-Cousins, P. Håkansson, S. S. Roy, L. J. Brown, R. C. D. Brown, G. Pileio, and M. H. Levitt, "A Nuclear Singlet Lifetime of More than One Hour in Room-Temperature Solution," *Angew. Chem. Int. Ed.* **54**, 3740–3743 (2015).
- ⁴⁵M. H. Levitt, "Long live the singlet state!" *Journal of Magnetic Resonance* **306**, 69–74 (2019).

Cross-correlation effects in the solution NMR of near-equivalent spin-1/2 pairs: Supplementary Material

James W. Whipham¹, Gamal A. I. Moustafa¹, Mohamed Sabba¹, Weidong Gong¹, Christian Bengs¹, and Malcolm H. Levitt^{1*}

*mhl@soton.ac.uk

¹Department of Chemistry, University of Southampton, SO17 1BJ, UK

August 22, 2022

arXiv:2208.09213v1 [physics.chem-ph] 19 Aug 2022

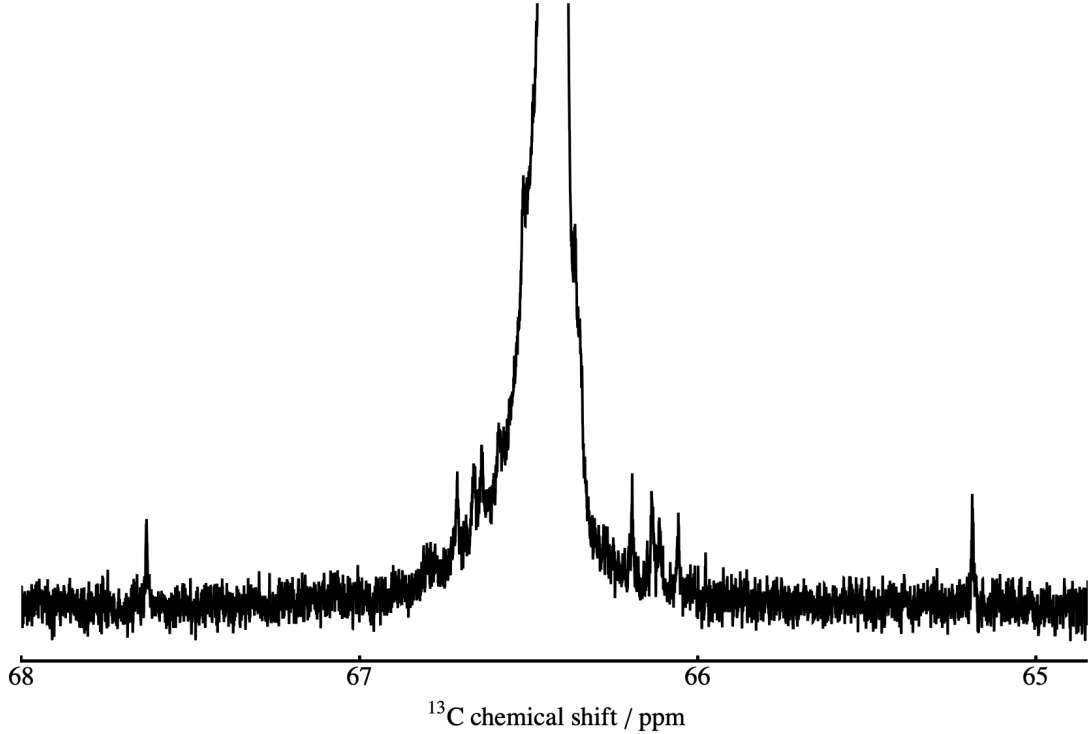


Figure 1: A portion surrounding the main doublet of the 700 MHz 90° pulse-acquire spectrum, showing the weak transitions at 65.19 and 67.63 ppm.

1 700 MHz Spectrum

A portion of the 90° pulse-acquire spectrum taken on a 700 MHz (16.4 T) spectrometer is shown in fig. 1, showing the weak outer-transitions at 65.19 and 67.63 ppm. Using table IV in the main text, we see that these peaks are associated with the $||S'_0\rangle\langle T'_{+1}|$ and $||T'_{-1}\rangle\langle S'_0|$ (-1) -quantum coherences, respectively.

The 700 MHz spectrum was also used to determine the isotropic J -coupling between the labelled nuclei as 214.15 Hz, by measuring the splitting between an outer peak and the associated inner-peak.

2 Relaxation Superoperator

2.1 Derivation

A spin Hamiltonian for interaction Λ may be written as a tensor product between a time-dependent spatial tensor and time-independent spin tensor. A convenient set of tensors to use are the *irreducible spherical tensor operators*, since these are eigenoperators of the Zeeman Hamiltonian commutation superoperator, leading to a simple expression in the corresponding interaction representation. For a rank- l interaction, we have,¹

$$H_l^\Lambda(t) = c^\Lambda \sum_{m=-l}^{+l} A_{lm}^{\Lambda*}(t) X_{lm}^\Lambda, \quad (1)$$

where c^Λ is a real constant specific to interaction Λ . Being Hermitian, we may also write,

$$\begin{aligned} H_l^\Lambda(t) &= H_l^{\Lambda\dagger} \\ &= c^\Lambda \sum_{m=-l}^{+l} A_{lm}^\Lambda(t) X_{lm}^{\Lambda\dagger}. \end{aligned} \quad (2)$$

Useful relations for components A_{lm} and X_{lm} are,

$$A_{lm}^* = (-1)^m A_{l-m}, \quad (3)$$

and,

$$X_{lm}^\dagger = (-1)^m X_{l-m}. \quad (4)$$

Then, using the eigenoperator relation,

$$[I_z, X_{lm}] = mX_{lm}, \quad (5)$$

the tensor components may be written in the interaction representation of the Zeeman interaction as,

$$\begin{aligned} \tilde{X}_{lm}(t) &= e^{i\hat{H}_Z t} X_{lm} \\ &= X_{lm} e^{im\omega_0 t}, \end{aligned} \quad (6)$$

where \hat{H}_Z is the Zeeman Hamiltonian commutation superoperator, $\hat{H}_Z = [H_Z, \dots] = \omega_0 [I_z, \dots]$. In a *Wangsness-Bloch-Redfield* (WBR) formalism, the relaxation superoperator takes the form,

$$\hat{\Gamma} = -\frac{1}{2} \int_{-\infty}^{+\infty} d\tau \overline{\hat{H}_{\text{fluc}}(t), \hat{H}_{\text{fluc}}(t+\tau)}. \quad (7)$$

From here, we simplify the expression. First, we have the liberty of setting $t = 0$ by assuming the noise in the system is stationary. This removes an exponential term in the interaction representation. Also, by neglecting the small dynamic frequency shifts, the correlation function has time-reversal symmetry and the integral may be taken from $-\infty$ to 0 while introducing a factor of two. We now write,

$$\hat{\Gamma} = - \int_{-\infty}^0 d\tau \overline{\hat{H}_{\text{fluc}}(0) \hat{H}_{\text{fluc}}(\tau)}. \quad (8)$$

$\hat{\Gamma}$ may be decomposed as a sum of auto- and cross-correlated relaxation superoperators. Simply,

$$\hat{\Gamma} = \sum_{\Lambda, \Lambda'} \sum_{l, l'} \hat{\Gamma}_{ll'}^{\Lambda\Lambda'}, \quad (9)$$

and using eq. (1) while utilising (2), $\hat{\Gamma}_{ll'}^{\Lambda\Lambda'}$ takes the form,

$$\hat{\Gamma}_{ll'}^{\Lambda\Lambda'} = -c^\Lambda c^{\Lambda'} \sum_{mm'} J_{ll'mm'}^{\Lambda\Lambda'}(\omega_0) \left[\hat{X}_{lm}^\Lambda \right]^L \left[\hat{X}_{l'm'}^{\Lambda'} \right]^L, \quad (10)$$

where the spectral density function is given by,

$$J_{ll'mm'}^{\Lambda\Lambda'}(\omega_0) = \text{Re} \int_{-\infty}^0 d\tau \overline{\left[A_{lm}^{\Lambda*}(0) \right]^L \left[A_{l'm'}^{\Lambda'}(\tau) \right]^L} e^{-im'\omega_0|\tau|}. \quad (11)$$

Here, the square brackets with the superscript L denote the laboratory frame. This is important since the spatial functions and spin tensors must be expressed in the same frame to legitimise the Hamiltonian they are associated with. However, the spatial functions are known in the molecule-fixed principal axis (P -) frame of the interaction in question, whereas the spin tensors are known in the space-fixed L -frame. Thus, we transform the spatial functions in the L -frame as a linear combination of functions in the diffusion (D -) frame using the properties of Wigner functions, before themselves being transformed as a linear combination of functions in the P -frame.

The relation to use is,

$$\left[A_{lm}(t) \right]^L = \sum_n \left[A_{ln} \right]^D D_{nm}^{(l)}(\Omega_{DL}(t)), \quad (12)$$

and the ensemble-averaged product in eq. (11) for the system becomes,

$$\begin{aligned} \overline{\left[A_{lm}^{\Lambda*}(0) \right]^L \left[A_{l'm'}^{\Lambda'}(\tau) \right]^L} &= \sum_{nn'} \overline{D_{mn}^{(l)}(\Omega_{LD}(0)) D_{m'n'}^{(l')*}(\Omega_{LD}(\tau))} \\ &\times \left[A_{ln}^{\Lambda*} \right]^D \left[A_{l'n'}^{\Lambda'} \right]^D, \end{aligned} \quad (13)$$

where the relation $D_{nm}^{(l)}(\Omega) = D_{mn}^{(l)*}(\Omega^{-1})$ is used, and $\Omega_{DL}^{-1} \equiv \Omega_{LD}$. The time-dependence of the spatial functions in the L -frame has been absorbed into the Wigner functions, since the D -frame is molecule-fixed. We then define the time-correlation function as that between the Wigner functions only, as,

$$\begin{aligned} G_{mm'nn'}^{ll'}(\tau) &= \overline{D_{mn}^{(l)}(\Omega_{LD}(0))D_{m'n'}^{(l')*}(\Omega_{LD}(\tau))} \\ &= \int \int d\Omega(0)d\Omega(\tau)D_{mn}^{(l)}(\Omega(0))D_{m'n'}^{(l')*}(\Omega(\tau)) \times P(\Omega(0))P(\Omega(\tau)|\Omega(0)), \end{aligned} \quad (14)$$

where Ω_{DL}^{-1} have been denoted simply by Ω in the second line for brevity, $P(\Omega(0)) = 1/(8\pi^2)$ and is the probability that the molecule hosting the spin system will be at orientation Ω at time $t = 0$, and $P(\Omega(\tau)|\Omega(0))$ is the *conditional probability* that the molecule will be at orientation $\Omega(\tau)$ at time $t' = t + \tau = \tau$ given that it was at orientation $\Omega(0)$ at time $t = 0$. From here, the notation and derivation is in similar vein of Huntress.^{2,3}

The time-derivative of the probability that the molecule will be at orientation $\Omega(\tau)$ at time τ , in the limit of a rigid molecule reorienting in random steps of small angular displacement, is given by the *Favro equation*,⁴

$$\frac{\partial}{\partial \tau} P(\Omega(\tau)) = -H_{\text{rot-diff}} P(\Omega(\tau)), \quad (15)$$

where $H_{\text{rot-diff}}$ is the *rotational-diffusion Hamiltonian*, which may be written in the form,

$$H_{\text{rot-diff}} = \mathbf{L} \bullet \mathbf{D} \bullet \mathbf{L} \quad (16)$$

where \mathbf{L} and \mathbf{D} are the quantum mechanical angular momentum operator and diffusion tensor, respectively. That is, the diffusion tensor describes the spatial aspect of the Hamiltonian in this case.

Favro shows that the solution to equation (15) is,⁴

$$P(\Omega(\tau)) = \int d\Omega(0)P(\Omega(0))P(\Omega(0)|\Omega(\tau)), \quad (17)$$

for which the conditional probability is,

$$P(\Omega(0)|\Omega(\tau)) = \sum_{\nu} \psi_{\nu}^*(\Omega(0))\psi_{\nu}(\Omega(\tau))e^{-E_{\nu}\tau}, \quad (18)$$

noindent where $\psi(\Omega)$ are eigenfunctions of $H_{\text{rot-diff}}$ with the associated eigenvalue E_{ν} . This solution is reliant on the boundary condition $P(\Omega(0)|\Omega(\tau \rightarrow 0)) = \delta(\Omega(0), \Omega(\tau))$, where $\delta(\Omega(0), \Omega(\tau))$ is the Dirac delta function.

If eq. (16) is written in the D -frame, it takes the form $H_{\text{rot-diff}} = \sum_i D_i L_i^2$ in which $i \in \{x, y, z\}$ and L_i have become the Cartesian angular momentum operators. This takes the form of the rigid-rotor Hamiltonian when considering the substitution $D_i \rightarrow \hbar^2/2I_i$, where I_i is the moment of inertia about principal axis i . Thus, (18) may be expanded in asymmetric-rotor eigenfunctions,

$$P(\Omega(\tau)|\Omega(0)) = \sum_{\nu, J, M} \psi_{\nu, M}^{J*}(0)\psi_{\nu, M}^J(\tau)e^{-E_{\nu}^J\tau}, \quad (19)$$

where,

$$\psi_{\nu, M}^J(t) = \sum_K a_{\nu, K}^J \phi_{K, M}^J \quad (20)$$

and $\phi_{K, M}^J$ are symmetric-rotor eigenfunctions which may be expressed in terms of Wigner functions and take the form,

$$\phi_{K, M}^J = (-1)^{M-K} \sqrt{\frac{2J+1}{8\pi^2}} D_{-M-K}^{(J)}(\Omega). \quad (21)$$

We then have all we need to obtain the time-correlation function and subsequently the spectral density function and relaxation superoperator. Inserting these eigenfunctions and probabilities into (33) and setting $\Omega \equiv \Omega_{LD}$ in (21),

$$\begin{aligned} G_{mm'nn'}^{ll'}(\tau) &= \frac{1}{8\pi^2} \sum_{\nu, J, M} (2J+1)e^{-E_{\nu}^J\tau} \\ &\times \int \int d\Omega_{LD}(0)d\Omega_{LD}(\tau)D_{mn}^{(l)}(\Omega_{LD}(0))D_{m'n'}^{(l')*}(\Omega_{LD}(\tau)) \\ &\times \left\{ \sum_K a_{\nu, K}^{J*} (-1)^{M-K} D_{-M-K}^{(J)*}(\Omega_{LD}(0)) \right\} \\ &\times \left\{ \sum_{K'} a_{\nu, K'}^J (-1)^{M-K'} D_{-M-K'}^{(J)}(\Omega_{LD}(\tau)) \right\}, \end{aligned} \quad (22)$$

and rearranging the expression, while using the orthogonality relation,

$$\int d\Omega D_{pq}^j(\Omega) D_{p'q'}^{j'}(\Omega) = \frac{8\pi^2}{2j+1} \delta_{jj'} \delta_{pp'} \delta_{qq'}, \quad (23)$$

the time correlation function simplifies to,

$$\begin{aligned} G_{mnn'}^l(\tau) &= \delta_{ll'} \delta_{mm'} G_{mm'nn'}^{ll'}(\tau) \\ &= \frac{(-1)^{n+n'}}{2l+1} \sum_{\nu} a_{\nu,n}^{l*} a_{\nu,-n'}^l e^{-E_{\nu}^l \tau}, \end{aligned} \quad (24)$$

where $l = l' = J$, $m = m' = -M$, $n = -K$ and $n' = -K'$.

From this, the spectral density becomes,

$$\begin{aligned} J_{lm}^{\Lambda\Lambda'}(\omega_0) &= \delta_{ll'} \delta_{mm'} J_{ll'mm'}^{\Lambda\Lambda'}(\omega_0) \\ &= \text{Re} \int_{-\infty}^0 d\tau \left[A_{lm}^{\Lambda*}(0) \right]^L \left[A_{lm}^{\Lambda'}(\tau) \right]^L e^{-im\omega_0|\tau|} \\ &= \sum_{nn'} \frac{(-1)^{n+n'}}{2l+1} \sum_{\nu} a_{\nu,n}^l a_{\nu,-n'}^l \left[A_{ln}^{\Lambda*} \right]^D \left[A_{ln'}^{\Lambda'} \right]^D \\ &\quad \times \text{Re} \int_{-\infty}^0 d\tau e^{-E_{\nu}^l \tau} e^{-im\omega_0|\tau|}. \end{aligned} \quad (25)$$

Performing the integral and inserting back into the relaxation superoperator, we have,

$$\begin{aligned} \hat{\Gamma}_l^{\Lambda\Lambda'} &= \delta_{ll'} \hat{\Gamma}_{ll'}^{\Lambda\Lambda'} \\ &= -c^{\Lambda} c^{\Lambda'} \sum_m J_{lm}^{\Lambda\Lambda'}(\omega_0) \left[\hat{X}_{lm}^{\Lambda} \right]^L \left[\hat{X}_{lm}^{\Lambda'\dagger} \right]^L, \end{aligned} \quad (26)$$

with,

$$\begin{aligned} J_{lm}^{\Lambda\Lambda'}(\omega_0) &= \sum_{nn'} \frac{(-1)^{n+n'}}{2l+1} \left[A_{ln}^{\Lambda*} \right]^D \left[A_{ln'}^{\Lambda'} \right]^D \\ &\quad \times \sum_{\nu} a_{\nu,n}^l a_{\nu,-n'}^l \frac{E_{\nu}^l}{E_{\nu}^{(l)2} + m^2 \omega_0^2}. \end{aligned} \quad (27)$$

This is the general case of an asymmetric-top molecule. To derive the case for a symmetric rotor with the P - and D -frames coincident (as in our model), we refer back to eq. (16), where we may write it in the D -frame as,

$$H_{\text{rot-diff}} = D_{\perp} (L_x^2 + L_y^2) + D_{\parallel} L_z^2 \quad (28)$$

where D_{\perp} and D_{\parallel} are rotational diffusion constants associated with axes perpendicular and parallel, respectively, with the spin chain.

Eq. (28) is of the same form as the rigid-rotor Hamiltonian for a symmetric-top. As such, the eigenfunctions and eigenvalues in eq. (18) are those of a quantum mechanical rigid-rotor:^{5,6}

$$\psi_{\nu}(t) \rightarrow \phi_{K,M}^J(t) \equiv (-1)^{M-K} \sqrt{\frac{2J+1}{8\pi^2}} D_{-M-K}^{(J)}(\Omega(t)) \quad (29)$$

$$E_{\nu} \rightarrow E_K^J \equiv D_{\perp} J(J+1) + K^2 (D_{\parallel} - D_{\perp}). \quad (30)$$

For our specific system, $J \equiv l = 2$ and $K = 0$. To see this, note that the only non-zero component for the dipole-dipole (DD) interaction is $[A_{20}^{\text{DD}}]^P = \sqrt{6}$ in the P -frame. The z -principal axis is defined as a vector connecting the two nuclei in question. We then assume this is coincident with the z -axis in the D -frame, with the x - and y -axes arbitrary. Writing, $D_{mn}^{(l)}(\alpha, \beta, \gamma) = e^{-im\alpha} d_{mn}^{(l)}(\beta) e^{-in\gamma}$ and assuming coincidence of the P - and D -frames (i.e. $\{\alpha, \beta, \gamma\} = \{0, 0, 0\}$), eq. (12) may be written,

$$\begin{aligned} [A_{20}^{\text{DD}}]^P &= \sum_n [A_{2n}^{\text{DD}}]^D d_{n0}^{(2)}(\beta = 0) \\ &= [A_{20}^{\text{DD}}]^D, \end{aligned} \quad (31)$$

where $d_{00}^{(2)}(\beta) = \frac{3\cos^2\beta-1}{2}$ is the only non-vanishing reduced Wigner function, and equates to unity for $\beta = 0$.

In general, the CSA P -frame will not be coincident with the DD P -frame. To simplify analytical expressions in the main text, however, they are assumed to be so for our system. Also, assuming cylindrical symmetry of the rigid-rod, the biaxiality parameters may be approximated as 0. Then the same relation holds for the CSA interaction; i.e. the only non-vanishing component of the spatial tensor is,

$$\left[A_{20}^{\text{CSA}}\right]^P = \left[A_{20}^{\text{CSA}}\right]^D. \quad (32)$$

Since $n = K$, the only non-vanishing term in the correlation function is then $E_0^{(2)} = 6D_{\perp}$, and related to the rotational correlation time $\tau_{\perp} \equiv (6D_{\perp})^{-1}$. We then see that rotational motion about the principal axis of inertia parallel to the rod does not modulate the interactions responsible for relaxation, and this is a consequence of the coincidence of the P - and D -frames, as well as the assumption that the molecule tumbles rigidly. The secularised time-correlation function for our system becomes,

$$G_{mm'nn'}^{ll'}(\tau) = \delta_{ll'}\delta_{mm'} \frac{(-1)^{n+n'}}{2l+1} e^{-\tau/\tau_{\perp}}. \quad (33)$$

The (-1) -QC subspace of the Liouvillian is given below. This shows that the off-diagonal elements are orders of magnitude smaller than the diagonal elements, and we, therefore, use the \mathbb{B}_Q basis and regard relaxation as a small perturbation when determining peak position. Also, since the mixing angle $\theta = \arctan(\omega_{\Delta}/\omega_J) = -0.075$, the \mathbb{B}_{ST} is used to simplify the λ_{\pm} expressions in the main text. The (-1) -QC subspace of the Liouvillian is,

$$\hat{\mathcal{L}}_{4 \times 4} = \begin{array}{c} \begin{array}{c} |S'_0\rangle\langle T'_{+1}| \\ |T'_{-1}\rangle\langle S'_0| \\ |T'_0\rangle\langle T'_{+1}| \\ |T'_{-1}\rangle\langle T'_0| \end{array} \end{array} \begin{pmatrix} |S'_0\rangle\langle T'_{+1}| & |T'_{-1}\rangle\langle S'_0| & |T'_0\rangle\langle T'_{+1}| & |T'_{-1}\rangle\langle T'_0| \\ -0.0852 + 1339.86i & 13.43 \times 10^{-5} & -3.16 \times 10^{-3} & 3.47 \times 10^{-3} \\ 13.43 \times 10^{-5} & -0.180 - 1339.86i & 3.65 \times 10^{-3} & -5.78 \times 10^{-3} \\ -3.16 \times 10^{-3} & 3.65 \times 10^{-3} & -0.168 + 5.68i & 94.16 \times 10^{-3} \\ 3.47 \times 10^{-3} & -5.77 \times 10^{-3} & 94.16 \times 10^{-3} & -0.338 - 5.68i \end{pmatrix} \text{s}^{-1}. \quad (34)$$

The real part is plotted is derived from the relaxation superoperator alone, and is plotted in figure 2.

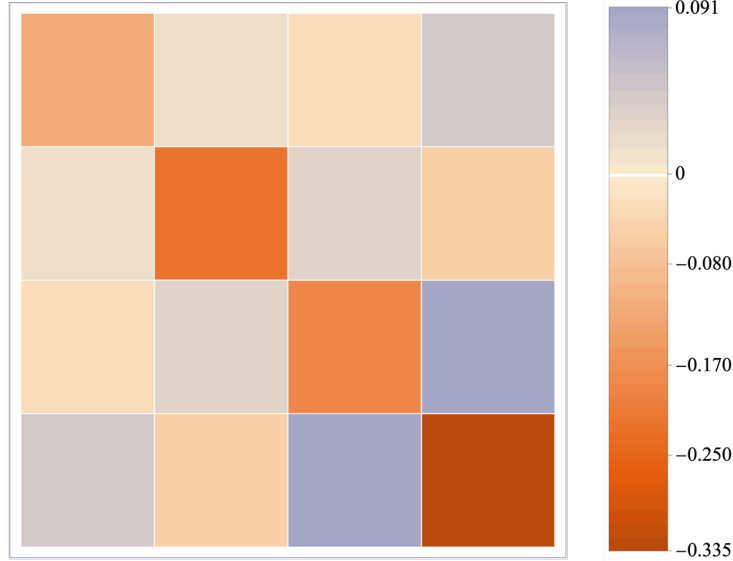


Figure 2: The (-1) -QC block of the real part of the Liouvillian in the \mathbb{B}_Q basis.

The computed magnetic shielding tensors are given in their respective P -frames by:

$$\sigma_1 = \begin{pmatrix} 258.73 & 0 & 0 \\ 0 & 41.59 & 0 \\ 0 & 0 & 38.65 \end{pmatrix} \text{ppm}, \quad (35)$$

and,

$$\sigma_2 = \begin{pmatrix} 258.64 & 0 & 0 \\ 0 & 42.25 & 0 \\ 0 & 0 & 38.90 \end{pmatrix} \text{ ppm.} \quad (36)$$

These are transformed to the chemical shift tensor δ by the relation,

$$\delta = \mathbb{I}\sigma_{\text{TMS}}^{\text{iso}} - \sigma, \quad (37)$$

where \mathbb{I} is the three-dimensional identity matrix, and $\sigma_{\text{TMS}}^{\text{iso}}$ is the isotropic component of the magnetic shielding tensor of tetramethylsilane, acting as a reference.

The shielding tensors (35) and (36) are transformed to their principal axis frames by diagonalisation. Then, the *Haerberlen convention*⁷ is used to define the anisotropy and biaxiality parameters, respectively, as,

$$\delta^{\text{CSA}} = \delta_{zz}^{\text{P}} - \delta^{\text{iso}} \quad (38)$$

and,

$$\eta = \frac{\delta_{xx}^{\text{P}} - \delta_{yy}^{\text{P}}}{\delta^{\text{CSA}}}, \quad (39)$$

with tensor components defined by,

$$|\delta_{zz}^{\text{P}} - \delta^{\text{iso}}| \geq |\delta_{xx}^{\text{P}} - \delta^{\text{iso}}| \geq |\delta_{yy}^{\text{P}} - \delta^{\text{iso}}|. \quad (40)$$

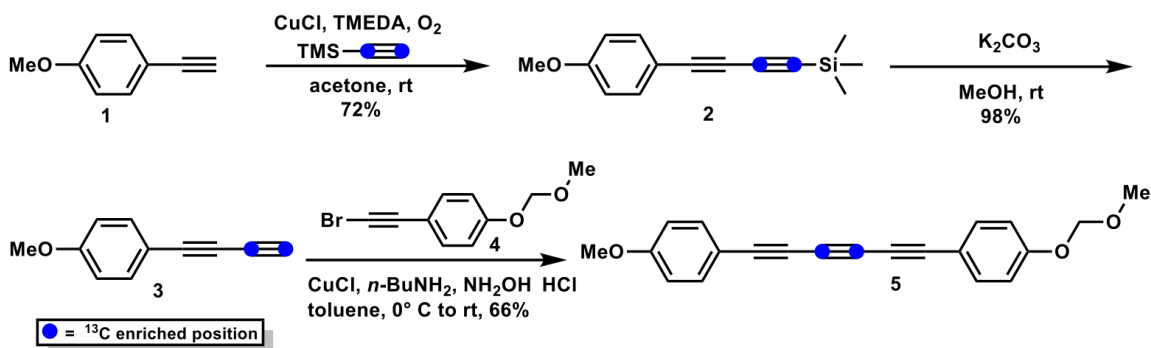
2.2 Estimation of τ_{\perp}

The correlation time was estimated using the experimental $T_1 = 2.24$ s value and the relation,

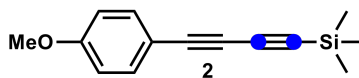
$$T_1^{-1} \simeq -\frac{(I_z|\hat{\Gamma}|I_z)}{(I_z|I_z)}, \quad (41)$$

and solving for τ_{\perp} .

3 Synthesis of Target Triyne 5



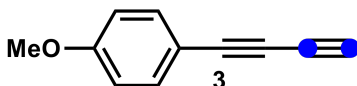
3.1 Synthesis of intermediate 2



To a stirred suspension of CuCl (41.6 mg, 0.42 mmol) in acetone (4 mL) was added tetramethylethylenediamine (TMEDA, 22.0 μL , 0.14 mmol), and the mixture was stirred for 30 minutes. Then, a mixture of 1-ethynyl-4-methoxybenzene **1** (264.3 mg, 2.0 mmol) and (trimethylsilyl)acetylene- ${}^{13}\text{C}_2$ (288 μL , 2.0 mmol) in

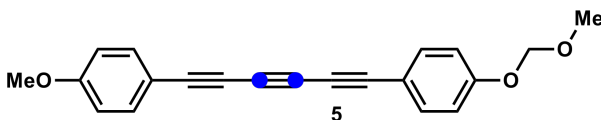
acetone (4 mL) was added slowly and bubbled with O₂ for 5 min. The reaction mixture was stirred for 2 h at room temperature, and then passed through a pad of silica gel. Then, the filtrate was concentrated under reduced pressure and the residue was purified by column chromatography using Et₂O/hexane (1:15) as eluent to afford compound **2** (332 mg, 72%) as a colorless oil. ¹H NMR (400 MHz, CDCl₃): δ 0.24 (dd, *J* = 2.5, 0.6 Hz, 9 H), 3.82 (s, 3 H), 6.84 (d, *J* = 9.4 Hz, 2 H), 7.44 (d, *J* = 9.4 Hz, 2 H). ¹³C{¹H} NMR (101 MHz, CDCl₃): δ 87.8 (d, *J* = 144.5 Hz, 1 C), 90.1 (d, *J* = 144.5 Hz, 1 C) (only ¹³C-enriched signals are shown). LRMS (ES+) *m/z* 231.1 (100%, [M + H]⁺).

3.2 Synthesis of intermediate **3**



A mixture of **2** (320 mg, 1.39 mmol), K₂CO₃ (384 mg, 2.78 mmol), MeOH (5 mL) and THF (5 mL) was stirred at room temperature for 1 h. Then, the reaction mixture was extracted with ethyl acetate and washed with brine. Evaporation of the solvent afforded diacetylene **3** (215 mg, 98%) as a colorless solid, which was used for the next step without further purification. ¹H NMR (400 MHz, CDCl₃): δ 2.46 (dd, *J* = 232.8, 77.8 Hz, 1H), 3.83 (s, 3H), 6.85 (d, *J* = 8.9 Hz, 1 H), 7.47 (d, *J* = 8.93 Hz, 2 H). ¹³C{¹H} NMR (101 MHz, CDCl₃): δ 68.03 (d, *J* = 192.20 Hz, 1 C), 71.04 (d, *J* = 191.47 Hz, 1 C) (only ¹³C-enriched signals are shown). LRMS (ES+) *m/z* 159.1 (100%, [M + H]⁺).

3.3 Synthesis of triyne **I**



To a solution of diacetylene **3** (197 mg, 1.26 mmol) in toluene (2.5 mL) at 0 °C were added CuCl (18.8 mg, 0.19 mmol), NH₂OH • HCl (26.3 mg, 0.38 mmol) and *n*-BuNH₂ (188 μL, 1.9 mmol) in order. Alkynyl bromide **4** (304 mg, 1.26 mmol) was diluted with 2.5 mL toluene and was added dropwise to the mixture. The reaction mixture was allowed to warm to room temperature and stir for 18 h. The reaction was quenched with H₂O and extracted with ether. The organic layer was washed with H₂O, brine and dried over MgSO₄. The solvent was evaporated, and the residue was purified by column chromatography using dichloromethane/hexane (1:2) as eluent to afford triyne **I** (263 mg, 66%) as a colorless solid. ¹H NMR (400 MHz, CDCl₃): δ 3.48 (s, 3 H), 3.84 (s, 3 H), 5.20 (s, 2 H), 6.86 (d, *J* = 8.0 Hz, 2 H), 7.00 (d, *J* = 8.0 Hz, 2 H), 7.50 (d, *J* = 8.9 Hz, 2 H), 7.49 (d, *J* = 8.9 Hz, 2 H). ¹³C{¹H} NMR (101 MHz, CDCl₃): δ 66.41 (d, *J* = 217.0 Hz, 1 C), 66.39 (d, *J* = 217.0 Hz, 1 C) (only ¹³C-enriched signals are shown). LRMS (ES+) *m/z* 317.1 (100%, [M + H]⁺).

References

- [1] S. A. Smith, W. E. Palke, and J. T. Gerig, "The Hamiltonians of NMR. part I," *Concepts Magn. Reson.* **4**, 107–144 (1992).
- [2] W. T. Huntress, "Effects of Anisotropic Molecular Rotational Diffusion on Nuclear Magnetic Relaxation in Liquids," *J. Chem. Phys.* **48**, 3524–3533 (1968).
- [3] W. T. Huntress, "The Study of Anisotropic Rotation of Molecules in Liquids by NMR Quadrupolar Relaxation," in *Advances in Magnetic and Optical Resonance*, Vol. 4, edited by J. S. Waugh (Academic Press, 1970) pp. 1–37.
- [4] L. D. Favro, "Theory of the Rotational Brownian Motion of a Free Rigid Body," *Phys. Rev.* **119**, 53–62 (1960).
- [5] R. N. Zare, *Angular Momentum: Understanding Spatial Aspects in Chemistry and Physics*, The George Fisher Baker Non-Resident Lectureship in Chemistry at Cornell University (Wiley, New York, 1988).

- [6] C. Wang, "Anisotropic-rotational diffusion model calculation of T1 due to spin-rotation interaction in liquids," *Journal of Magnetic Resonance* (1969) **9**, 75–83 (1973).
- [7] U. Haeberlen, *High Resolution NMR in Solids: Selective Averaging*, *Advances in Magnetic Resonance* : Supplement No. 1 (Academic Press, New York, 1976).